UV Sensitivity to Changes in Ozone, Aerosols, and Clouds in Seoul, South Korea

WOOGYUNG KIM, JHOON KIM, SANG SEO PARK, AND HI-KU CHO

Global Environment Laboratory/Department of Atmospheric Sciences, Yonsei University, Seoul, South Korea

(Manuscript received 5 February 2013, in final form 19 September 2013)

ABSTRACT

The total ozone (O_3) and aerosol optical depth (AOD) at 320 nm have been observed from the ultraviolet (UV) measurements made at Yonsei University in Seoul, South Korea, with Dobson and Brewer spectrophotometers, respectively, during 2004–10. The daily datasets are analyzed to show the sensitivities of UV radiation to changes in O_3, AOD, and cloud cover (CC) together with global solar radiation (GS), including the long-term characteristics of surface UV irradiance in Seoul. The UV sensitivities show that 1% increases of O_3 and AOD relative to their reference values under all- and clear-sky conditions similarly manifest as 1–1.2% and 0.2% decreases of both daily erythemal UV (EUV) and total UV (TUV) irradiance at the ground level except for TUV sensitivity to O_3 (~0.3%). Those UV sensitivities to CC and GS changes are associated with a 0.12% decrease and 0.7% increase, respectively, in fractional UV changes. The trends show that the positive trends of O_3 (+7.2% decade^{-1}), AOD (+22.4% decade^{-1}), and CC (+52.4% decade^{-1}) induce negative trends in EUV (−8.4% decade^{-1}) and TUV (−2.5% decade^{-1}), in both UV (−4.7% decade^{-1}), and in EUV (−6.3% decade^{-1}) and TUV (−6.8% decade^{-1}), respectively. On the basis of the multiple linear regression analyses, it is found that UV sensitivity to O_3 is relatively high in the forcing factors, but the contributions of the UV forcing factors to the daily variability and the range of UV disturbances due to the variability of the forcing factors are affected more by AOD than by O_3 and CC in both UV fractional changes.

1. Introduction

It is well known that the UV radiation reaching the earth's surface is damaging to the human body and the ecosystem, and that the ozone layer in the lower stratosphere absorbs a substantial fraction of the harmful UV-B radiation (280–320 nm) from the sun. On the way through the atmosphere, solar radiation is absorbed and scattered by molecules, aerosols, and clouds. In the UV-B range, ozone is the most effective molecule for absorption. Absorption and scattering by aerosols are of minor importance in the UV-B range compared with absorption by ozone and molecular scattering. Attenuation by clouds is also strongly pronounced in the UV-B range; however, it varies strongly with the type and spatial distribution of the clouds (Blumthaler 1993). Many studies have investigated the effect of ozone on surface UV radiation (Cho et al. 1998; Madronich 1992; McKenzie et al. 1991; Stolarski et al. 1992), but relatively few studies have considered the effects of aerosols and clouds. Since the industrial revolution, the amount of aerosol in the atmosphere has increased. Thus, there has been increasing interest in investigating the effects of aerosol on surface UV-B variations (Arola et al. 2003; Kazadzis et al. 2007; Krzyscin and Puchalski 1998). Liu et al. (1991) recognized the importance of aerosols on the surface UV irradiance. The effect of clouds on UV radiance has been quantified in a few studies (e.g., Antón et al. 2012a; Bais et al. 1993; Calbó et al. 2005; Josefsson and Landelius 2000; Lubin and Frederick 1991; Schafer et al. 1996).

Over a short time scale (day to day and month to month), the ozone impact on UV surface irradiance has been well documented (McKenzie et al. 1991, 1994). The concept of power radiation amplification factors (power RAF) has been applied to the analysis of not only ozone (Antón et al. 2008; Booth and Madronich 1994; Madronich 1993; Micheletti et al. 2003) but also aerosols (Kim et al. 2013). Kim et al. (2013) calculated the RAFs due to total ozone (O_3) and aerosol optical depth (AOD) as a function of solar zenith angle (SZA) and O_3 (or AOD) under all- and clear-sky conditions suggesting cloud effects in Seoul, South Korea (37.57°N, 126.98°E), with the measurement data from 2004 to 2008. The overall mean RAF (AOD, SZA) due to O_3

Corresponding author address: Jhoon Kim, Global Environment Laboratory, Dept. of Atmospheric Sciences, Rm. 545 Science Hall, 50 Yonsei-Ro, Seodaemoon-gu, Seoul 120-749, South Korea.
E-mail: jkim2@yonsei.ac.kr

DOI: 10.1175/JAMC-D-13-052.1

shows that a 1% decrease in O_3 forces an 1.18% increase in the erythemal UV (EUV) irradiance with the maximum range of 0.67%–1.74% depending on SZA (40°–70°) and AODs (<4.0) under both clear- (cloud cover < 2.5 tenths) and all-sky conditions. A similar analysis of the RAF (O_3, SZA) due to AOD shows that, on average, a 1% increase in AOD forces a decrease of 0.29% in EUV irradiance with the maximum range of 0.18%–0.63% depending on O_3 and SZAs. Kim et al. (2013) also found a difference between clear- and all-sky RAFs, suggesting cloud effects. Krzyscin and Puchalski (1998) showed a 0.15% decrease in UV radiation with respect to a 1% increase of AOD at 550 nm in Belsk, Poland.

This study focused on the relationship between UV and parameters other than ozone (such as aerosols and clouds) over long time scales (years and decades). To estimate the cloud effect, Kim et al. (2011) calculated that transmissions of radiation through clouds under cloudy-sky conditions (cloud cover ≥ 7.5 tenths) were 58%, 55%, and 40% for EUV, total UV (TUV), and global solar radiation (GS), respectively. Clouds under all-sky conditions (where average cloud cover is 5, in tenths) reduced the EUV and TUV to about 25% of the clear-sky values, and reduced GS to 31%. Schafer et al. (1996) reported the UV-B transmissions for some typical cloud covers at an SZA of 50° at Black Mountain, North Carolina, in the United States.

To better understand the health risks of UV damage, it is important not only to quantify the extent of ozone changes and their impact on surface UV-B variations but also to view such changes from within the context of natural variability. This requires a quantitative evaluation of the effects of factors on surface UV-B level, such as the reduction of incoming solar radiation by clouds and aerosols in the atmosphere and the total amount of ozone along the radiation path. This study aims to show UV sensitivities to changes in O_3, AOD, cloud cover (CC), and GS irradiance together with their contributions to UV variability on the basis of multiple linear regression analyses in a comparison between EUV and TUV irradiance. Trends in the UV forcing factors and trends in the UV irradiance caused by these forcing factors are also evaluated with the time series of fractional deviation of daily UV irradiance from the reference values obtained by a superposition of sinusoids fitted to the daily data in this study. Changes in the amount of UV radiation reaching the earth's surface depend mainly on changes in the UV forcing factors of ozone, atmospheric turbidity (aerosols), and clouds, except for geometric factors such as pathlength of sun rays through the atmosphere (e.g., solar zenith angle) and surface albedo. However, here, as an SZA effect, a seasonal dependence affecting surface UV is evaluated. The effect of the albedo change can be dismissed, since the measurements site is surrounded by buildings and thus maintains almost the same albedo throughout the year, although occasional snow cover in winter could affect the values. Therefore, this study considers three variables as the UV forcing factors affecting the variation of UV radiation: total ozone, AOD (320 nm), and cloud amount from year-round and seasonal regression models. The regression model provides an efficient tool to study the short-term and long-term changes in UV irradiance related to forcing by O_3, atmospheric turbidity, and cloud cover (Krzyscin 1996). In addition, the maximum variations of EUV irradiance due to changes in extremes of the O_3 and AOD have been compared with the radiative transfer model calculations.

2. Instrumentation and data

The Global Environment Laboratory at Yonsei University in Seoul (37.57°N, 126.98°E) has carried out the ozone layer monitoring program in the framework of the Global Ozone Observing System of the World Meteorological Organization (WMO/GAW/GO3OS Station 252) since May of 1984. Daily measurements of total ozone and the vertical distribution of ozone have been made with a Dobson spectrophotometer (Beck 124) (-Komhyr 1980), which estimates total ozone to within ±2% accuracy, on the roof of Science Hall on the Yonsei University campus. From 2004 through 2006, major parts of the manual operations were automated with new hardware including a step motor, rotary encoder, controller, and visual display to measure the total ozone amount and vertical ozone amount through the Umkehr method and to calibrate the instrument by mercury and standard lamp tests. This system takes full advantage of the Microsoft Corp. Windows interface and information technology for adaptability to the latest Windows personal computer and flexible data-processing system. This automatic system also utilizes the card slot of a desktop personal computer to control various types of boards in the driving unit for operating the Dobson spectrophotometer and testing devices. Thus, subjective human error and individual differences are eliminated by automating most of the manual work both in instrument operation and in data processing. Therefore the ozone data quality has been distinctly upgraded since the automation of the Dobson instrument. The calibration history of the instrument has been well documented by Kim et al. (2007).

A SCI-TEC Instruments, Inc., model MKIV Brewer spectrophotometer (#148) has also been in routine operation since October of 1997 at the same site to

measure the direct UV spectral solar beam at five wavelengths (306.3, 310.1, 313.5, 316.7, and 320.1 nm) for ozone (O_3), sulfur dioxide (SO_2), and aerosol. These direct-spectra measurements are performed in intervals of 5–10 min. The AOD at a given wavelength is calculated as the residual optical depth after subtracting from the total atmospheric optical depth due to molecular scattering and the O_3 and SO_2 absorption. The Brewer AOD retrieval based on the methodology introduced by previous studies (Cheymol and De Backer 2003; Grobner et al. 2001; Meleti and Cappellani 2000) is installed in the Brewer #148. The Brewer is designed for ±1% accuracy in direct-sun total column ozone measurements and is mounted on a solar tracker to measure the direct solar beam. In addition, the Brewer instrument enables measurement of global UV spectra (290–363 nm with a 0.5-nm interval) irradiance on horizontal surface. The irradiance at each wavelength is integrated to produce a total ultraviolet irradiance (290–363 nm: TUV) and an erythemal UV-B value (290–325 nm: EUV) weighted to the Diffey actions spectrum (McKinlay and Diffey 1987). Therefore, the integrated irradiance values represent both EUV and TUV in the units of joules per meter squared. Typically from one to four such measurements are performed every hour throughout the daytime from sunrise to sunset. The number of measurements is about 30 times per day for winter and up to 60 times per day for summer. The instrument is mounted in an insulated weatherproof enclosure (painted white). Several lamp tests of the Brewer are performed regularly each day to ensure that the instrument is in good condition. The wavelength calibration of the instrument is ensured before each scene by using an internal mercury lamp, and absolute calibration is achieved by an external lamp test for comparison to 50-W standard lamps (tungsten halogen) traceable to the standards of the National Institute of Standard and Technology. A standard lamp is used as a reference for the relative sensitivity. Two values from this test corresponding to the values of ozone (ratio 6) and sulfur dioxide (ratio 5), which should stay consistent within ±5%, are recorded daily and compared with those from previous tests. Apart from the above calibrations, the Brewer #148 was regularly recalibrated for UV, ozone, and aerosol against the traveling standard Brewer #017 by the visiting K. Lamb (International Ozone Service, Canada) between 2004 and 2011 at Yonsei University, Seoul, on 10–16 March 2004, 24–25 February 2006, 24 October–3 November 2007, 16 October 2009, and 21 November 2011. The total ozone data from Dobson measurements are available for most of the period. When the Dobson observation was unavailable, the data gap was filed in by Brewer data correction by using regression analysis between the two other periods. Data for the daily cloud amount and global solar radiation are available from the Seoul meteorological station of the Korea Meteorological Administration located about 3 km east of the present site. The GS is measured by the Kipp & Zonen CM21 pyranometer, with a wavelength range of 305–2800 nm. Data were recorded for an average of 1 min using Campbell Scientific CR21X dataloggers and were archived as hourly integrals. The daily values are the hourly totals of the 24 h of each day in units of watts per meter squared. The CC is observed visually and expressed as tenths of the sky covered by clouds according to WMO standards. The daily cloud amount is obtained by averaging eight times per day (0300–0000 LST). This study uses the daily data for the period 2004–10.

3. Statistical models

The EUV and TUV irradiances are significantly correlated with four variables in the fractional deviation values (O_3, AOD, CC, and GS) as UV forcing factors listed in Table 1. All the coefficients r indicate statistical significance ($P < 0.05$), although the correlation between TUV and O_3 is a relatively low value of 0.058 ($P = 0.022$) for weak ozone absorption of TUV irradiance. Cho et al. (2008) explained the contributions of air temperature, clouds, and specific humidity to the variations of downward longwave radiation with the multiple regression model. Similarly, based on the correlations of these variables (O_3, AOD, and CC) with the EUV and TUV irradiances, two multiple linear regression models have been developed to evaluate the relative contributions of each individual forcing factors to the EUV and UV variability. The models take into account the UV variations induced by the three UV forcing factors. The regression coefficients for the model in the fractional deviation of the UV forcing factors from the reference correspond to the linear RAFs (Booth and Madronich 1994; Krzyscin and Puchalski 1998) and the UV sensitivity to changes in the UV forcing factors (Micheletti et al. 2003), which is defined as the percent changes of the UV irradiance divided by the percent changes of UV forcing factors.

Figure 1 shows a time series of daily parameters used in this study (EUV, TUV, O_3, AOD, CC, and GS); the solid line represents a pattern of the reference values obtained by superposition of sinusoids fitted to the daily data in the period 2004–10. Each sinusoid was obtained by harmonic analysis (Wilks 2006). The following multiple linear regression models are proposed to explain most of the observed variations of the daily UV irradiance. Model (1) includes three independent variables (UV forcing factors) as follows:

TABLE 1. Individual coefficients of partial correlation and beta coefficients for UV forcing factors: O_3, AOD, CC, and GS. Here $P = 0.02$ for r, and $P = 0.000$ for β.

Dependent variables	Independent variables (forcing factors)	Coefs of partial correlation r	Beta coef β	Significance level (P value)
		All sky; $N = 1214$		
EUV	O_3	−0.309	−0.364	0.000
	AOD	−0.568	−0.441	0.000
	CC	−0.442	−0.285	0.000
	GS	0.711	0.719	0.000
TUV	O_3	−0.058	−0.124	0.022
	AOD	−0.655	−0.490	0.000
	CC	−0.567	−0.350	0.000
	GS	0.820	0.822	0.000
		Clear sky (CC < 2.5 tenths); $N = 442$		
EUV	O_3	−0.412	−0.435	0.000
	AOD	−0.568	−0.586	0.000
	GS	0.559	0.596	0.000
TUV	O_3	−0.059	−0.086	0.016
	AOD	−0.667	−0.670	0.000
	GS	0.594	0.603	0.000

$$\frac{(\mathrm{UV}_i - \mathrm{UV}_i^*)}{\mathrm{UV}_i^*} = a + b \times \frac{(\mathrm{O}_{3_i} - \mathrm{O}_{3_i}^*)}{\mathrm{O}_{3_i}^*} + c \times \frac{(D_i - D_i^*)}{D_i^*} + d \times \frac{(\mathrm{CC}_i - \mathrm{CC}_i^*)}{\mathrm{CC}_i^*} + \varepsilon_i, \tag{1}$$

where UV_i is the UV irradiance on day i; O_{3_i} is the total ozone amount; D_i is the aerosol optical depth at 320 nm; CC_i is the cloud cover; X_i^* indicates the reference value on day i for any variable X; a, b, c, and d are the model constants to be determined by an ordinary least squares fit; and ε_i is the noise term. The regression coefficients b, c, and d correspond to the linear RAFs due to O_3, AOD, and CC (Booth and Madronich 1994), and the UV sensitivity (Micheletti et al. 2003). The predictor variables of the model are chosen to account for the impact of O_3, AOD, and CC on the surface UV irradiance. Model (2) (which includes two independent variables) is proposed to explain the variation of UV irradiance as follows:

$$\frac{(\mathrm{UV}_i - \mathrm{UV}_i^*)}{\mathrm{UV}_i^*} = a' + b' \times \frac{(\mathrm{O}_{3_i} - \mathrm{O}_{3_i}^*)}{\mathrm{O}_{3_i}^*} + c' \times \frac{(\mathrm{GS}_i - \mathrm{GS}_i^*)}{\mathrm{GS}_i^*} + \varepsilon_i', \tag{2}$$

where GS_i is the global (direct plus diffuse) irradiance (GS) on day i. Here a' is a constant, and b' and c' are the regression coefficients (i.e., linear RAFs). The GS is used as a new predictor variable in model (2) because GS depends on characteristics of both clouds and aerosols. This model is constructed to compare the impact of ozone on the UV irradiance with that due to combined cloud and aerosol.

The two multiple linear regression models mentioned above are examined for EUV and TUV irradiance, respectively. The regression coefficients and constants in models (1) and (2) are calculated using 1214 daily data points (i.e., about 50% of all possible days for the period of April 2004–December 2010). Year-round and seasonal models are run separately for the EUV and TUV irradiances. The regression coefficients (RAFs and UV sensitivity) are analyzed together with an estimate of G_X, that is, the mean range of factor X disturbances in the UV irradiance. The term G_X is defined as the standard deviation of X multiplied by the absolute value of the regression coefficients pertaining to this factor (Krzyscin and Puchalski 1998), which means changes in UV irradiance due to the factor X within the range $\pm G_X$. The term P_X is the individual contribution defined as the partial correlation coefficient r of X multiplied by the beta coefficient β, which is the standardized regression coefficient. Table 2 shows the percent of the total variance explained by a determination coefficient R^2 of the multiple regression models and the standard error of noise (Res).

4. Results and discussion

The inverse effects of surface UV irradiance on ozone, aerosols, and clouds in short-term and long-term changes are demonstrated by measurements and the theory for their absorption and scattering processes (e.g., Herman 2010; Kyle 1991; Liou 1992; Madronich 1993; Madronich et al. 1998; McKenzie et al. 1991).

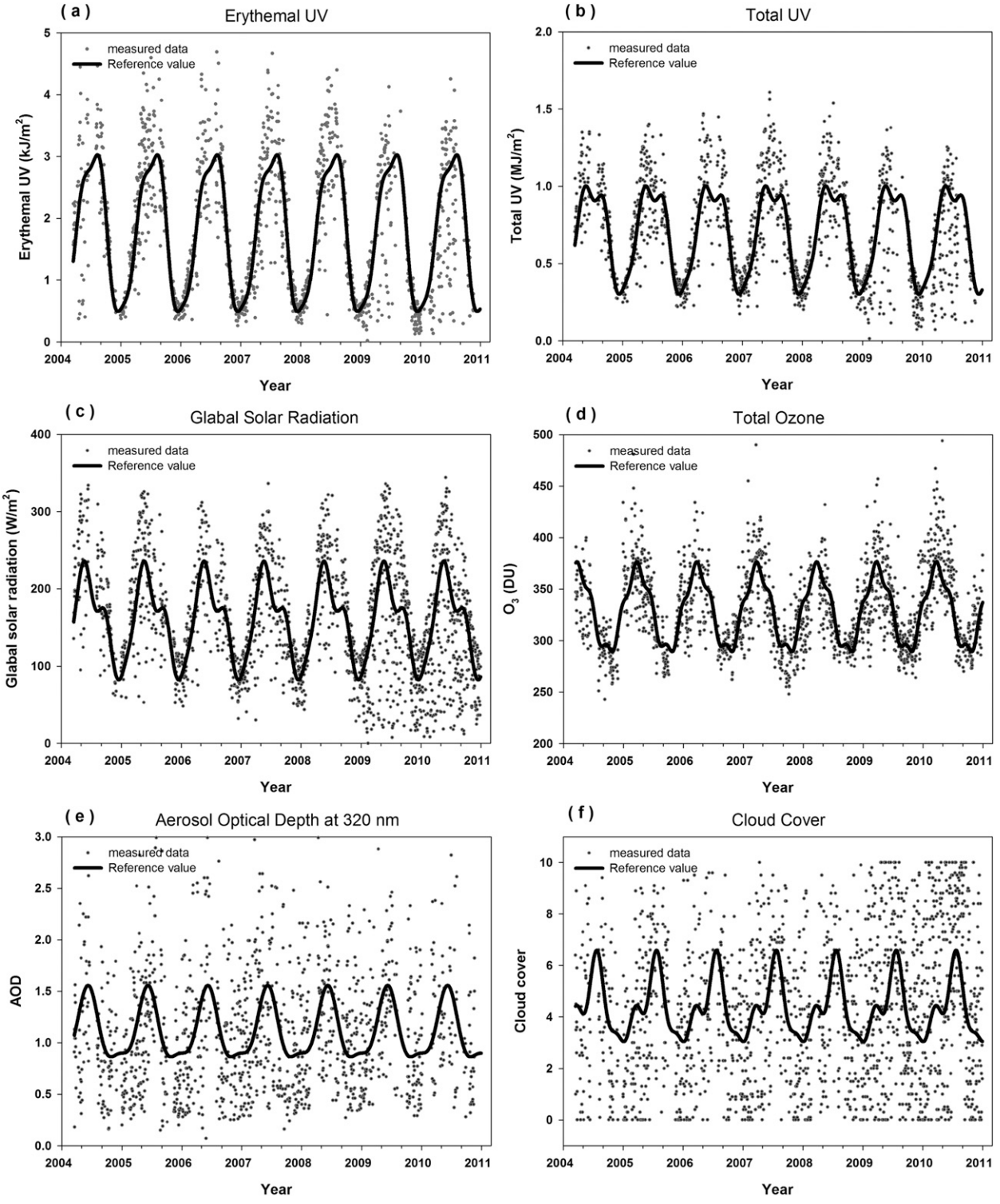

FIG. 1. The time series used as input for the multiple regression models. (a) EUV and (b) TUV irradiance at the ground level under all-sky conditions, (c) GS, (d) O_3 from the Dobson spectrophotometer, (e) AOD at 320 nm, and (f) CC. The solid lines represent the reference time series obtained from the least squares fit to the time series shown. The data points (daily value) are shown if all variables were measured.

TABLE 2. Regression coefficients a, b, c, and d (linear RAFs) and their standard errors by the multiple regression model used. The G_X is the range of the disturbances and P_X is individual contributions of UV variations due to the UV forcing factors (O_3, AOD, CC, and GS). The percentage of variance R^2 is that explained by the regression model. Res indicates variance of the model noise. Here, N is the number of data.

	Model (1)			Model (2)	
	EUV	TUV		EUV	TUV
			Year-round model (all sky); $N = 1214$		
$a \times 100$	2.24 ± 0.54	2.73 ± 0.46	$a' \times 100$	−0.9 ± 0.4	−0.3 ± 0.4
b (O_3)	−1.16 ± 0.07	−0.35 ± 0.06	b' (O_3)	−1.04 ± 0.06	−0.22 ± 0.05
c (cloud)	−0.12 ± 0.01	−0.13 ± 0.01	c' (GS)	0.71 ± 0.02	0.71 ± 0.01
d (AOD)	−0.21 ± 0.01	−0.21 ± 0.01			
G_{O_3} (%)	9.4	2.8	G_{O_3} (%)	8.5	1.8
G_{cc} (%)	7.4	8.0	G_{gs} (%)	18.6	18.8
G_{aod} (%)	11.4	11.2			
P_{O_3} (%)	11.2	0.7	P_{O_3} (%)	10.1	0.5
P_{cc} (%)	12.6	19.9	P_{gs} (%)	51.1	67.4
P_{aod} (%)	25.0	32.1			
R^2 (%)	48.8	52.7	R^2 (%)	61.2	67.9
Res (%)	3.4	2.5	Res (%)	2.6	1.7
			Winter model; $N = 320$		
$a \times 100$	1.2 ± 0.8	2.4 ± 0.8	$a' \times 100$	−1.3 ± 0.6	0.3 ± 0.6
b (O_3)	−1.3 ± 0.09	−0.33 ± 0.08	b' (O_3)	−1.26 ± 0.07	−0.26 ± 0.07
c (cloud)	−0.07 ± 0.01	−0.08 ± 0.01	c' (GS)	0.73 ± 0.03	0.7 ± 0.03
d (AOD)	−0.24 ± 0.02	−0.22 ± 0.02			
G_{O_3}, %	11.7	2.9	G_{O_3}, %	11.3	2.3
G_{cc}, %	5.1	5.9	G_{gs}, %	18.4	17.5
G_{aod}, %	12.9	12.0			
P_{O_3}, %	17.9	−0.8	P_{O_3}, %	17.2	−0.6
P_{cc}, %	10.3	17.5	P_{gs}, %	58.9	70.9
P_{AOD}, %	34.2	43.0			
R^2, %	62.0	59.4	R^2, %	76.0	70.0
Res, %	1.9	1.7	Res, %	1.2	1.3
			Summer model; $N = 245$		
$a \times 100$	0.7 ± 1.4	1.8 ± 1.2	$a' \times 100$	−3.4 ± 1.1	−1.8 ± 1.0
b (O_3)	−1.6 ± 0.22	−1.16 ± 0.19	b' (O_3)	−1.3 ± 0.18	−0.83 ± 0.16
c (cloud)	−0.24 ± 0.03	−0.27 ± 0.03	c' (GS)	0.69 ± 0.04	0.69 ± 0.03
d (AOD)	−0.20 ± 0.03	−0.18 ± 0.02			
G_{O_3}, %	9.9	7.1	G_{O_3}, %	8.0	5.1
G_{cc}, %	10.1	11.4	G_{gs}, %	19.9	19.7
G_{aod}, %	10.3	9.7			
P_{O_3}, %	13.9	8.6	P_{O_3}, %	11.3	6.2
P_{cc}, %	15.6	22.7	P_{gs}, %	53.3	60.7
P_{AOD}, %	19.2	20.0			
R^2, %	48.0	50.8	R^2, %	64.0	66.6
Res, %	4.1	3.3	Res, %	2.8	2.2
			Year-round model (clear sky; CC < 2.5 tenths)l; $N = 442$		
$a \times 100$	9.1 ± 0.8	9.8 ± 0.8	$a' \times 100$	−2.2 ± 1.3	0.7 ± 1.3
b (O_3)	−1.20 ± 0.09	−0.20 ± 0.08	b' (O_3)	−1.24 ± 0.09	−0.25 ± 0.09
d (AOD)	−0.29 ± 0.02	−0.29 ± 0.02	c' (GS)	0.77 ± 0.04	0.67 ± 0.04
G_{O_3}, %	9.2	1.6	G_{O_3}, %	9.7	2.0
G_{aod}, %	12.4	12.1	G_{gs}, %	12.6	11.1
P_{O_3}, %	17.9	0.5	P_{O_3}, %	19.0	0.6
P_{AOD}, %	33.3	44.7	P_{gs}, %	33.3	35.8
R^2, %	51.2	45.2	R^2, %	52.3	36.5
Res, %	2.2	1.9	Res, %	2.1	2.2

a. Short-term variations

The results presented in Table 2 show that all the regression coefficients for EUV and TUV models are statistically significant at a level $P = 0.000$. Under all-sky conditions, for the year-round model (1) including three variables, the regression coefficients b, c, and d corresponding to the linear RAFs (UV sensitivities) due to O_3, AOD, and cloud cover (O_3 RAF, AOD RAF, and CC RAF) are -1.16 ± 0.07, -0.21 ± 0.01, and -0.12 ± 0.01, respectively as listed in Table 2. The linear O_3 and AOD RAFs are comparable to the power RAFs (Madronich 1993) of 1.18 for ozone and 0.29 for AOD (Kim et al. 2013). The linear O_3 RAF for TUV is about 3 times smaller than that for EUV, whereas the RAFs for cloud and AOD are comparable to those for EUV irradiance. For the year-round model (2) including two variables, the O_3 RAF for TUV is about 4 times smaller than that for the EUV, while the GS RAF for TUV is almost consistent with the EUV value. Thus the GS change of 1% is associated with a change of 0.71% for both the UV irradiances. Moreover, these values correspond with those obtained by Krzyscin (1996). These sensitivities to the UV forcing factors show a negligible seasonal dependence.

The respective mean range of daily EUV disturbances due to changes of the O_3, AOD, and CC is about $\pm 9\%$, $\pm 11\%$, and $\pm 7\%$ relative to the climatological EUV level, whereas that of the TUV is about $\pm 3\%$, $\pm 11\%$, and $\pm 8\%$. In case of GS, relatively large ranges of about $\pm 19\%$ occur for both UVs. Accordingly, the ratio between the mean range of UV disturbances due to aerosol variability and that due to total ozone ($G_{\mathrm{aod}}/G_{\mathrm{O_3}}$) is 1.21 and 4.00 in the EUV and TUV, respectively. The ratio between the mean range of UV disturbances due to CC variability and that due to total ozone ($G_{\mathrm{cc}}/G_{\mathrm{O_3}}$) is 0.79 and 2.86 in the EUV and TUV, respectively. The ratio between the mean range of UV disturbances due to changes of the GS and that due to O_3 ($G_{\mathrm{gl}}/G_{\mathrm{O_3}}$) is 2.19 and 10.4 in the EUV and TUV, respectively. Similar values for the range of UV disturbances due to O_3 variability are found in both models (1) and (2). In Table 2, the coefficient of multiple determination R^2 indicates the proportion of the variance in the dependent variable $(\mathrm{UV}_i - \mathrm{UV}_i^*)/\mathrm{UV}_i^*$. Model (1) for EUV explains only 48.8% of all the variance of the UV fractional changes, whereas model (1) for TUV explains 52.7% of the variance. Model (2) accounts for 61.2% of variance for EUV and the 67.9% for TUV. Among the 49% explained by model (1) for EUV, relative contribution P_X of each individual variable to the variation of daily EUV fractional deviation was found to be 11.2%, 25.0%, and 12.6% for O_3, AOD, and CC, respectively. Among the 52.7% explained by model (1) for TUV, the relative contribution P_X of each individual variable was found to be 0.7%, 32.1%, and 19.9%, respectively. As a result, the contributions of the UV forcing factors to daily UV variability are affected more by AOD than by O_3 and CC in both UV variations. From the data given in Table 2, the EUV model (2) for two variables of O_3 and GS together explained 61.2% of all the variance, with individual contribution P_X of 10.1% and 51.1% for total ozone and global solar irradiance, respectively. For TUV irradiance, two variables together explained 67.9% of all the variance with P_X, with individual contribution of 0.5% and 67.4% for the O_3 and GS irradiance, respectively. Thus the O_3 effect on TUV variability is relatively low for weak O_3 absorption.

In view of the above results, it is likely that part of the variation in the UV irradiance, which is not explained by the UV forcing factors considered in this study, could be better explained by the addition of the new factors for which data might be unavailable in this climatological study. For example, new factors such as O_3 profile, air pollution, and clouds could change the UV irradiance. In particular, for clouds, UV can be enhanced under partly cloudy conditions when the sun is not obscured because of reflections from the sides of clouds depending on morphology (Antón et al. 2012b; Jung et al. 2011; Mims and Frederick 1994; Sabburg and Wong 2000). Therefore, the CC could not satisfactorily represent the cloud effects as a variable in UV variations.

The UV sensitivities to changes of the forcing factors obtained from the year-round and seasonal models can be summarized as follows. For O_3, the EUV sensitivity coefficients vary from around -1.0 for both spring and autumn to -1.6 for summer, whereas the TUV coefficients vary from a negligibly small value (0.03) for autumn to -1.16 for summer. For clouds, the EUV and TUV coefficients vary from around -0.1 for both autumn and winter to -0.27 for summer. For AOD, both EUV and TUV coefficients are similar with a value of 0.21 for all seasons. For a GS, both EUV and TUV coefficients vary from 0.65 for autumn to 0.78 for spring. A negligibly small difference between EUV and TUV is found in the sensitivity to cloud and aerosol changes for each season. The coefficients of the determination (R^2) for seasonal EUV and TUV regression models show that the EUV and TUV increased to 0.62 and 0.59 for winter but decrease to 0.48 and 0.51 for summer compared to year-round value, respectively. Table 2 shows the results of similar regression analysis for the sensitivity under clear-sky conditions. The difference in the sensitivity between all-sky and clear-sky conditions is negligible and within the margin of around errors.

TABLE 3. Annual averages, trends, and forced trends of the UV forcing factors for the period 2004–10.

Variables	Annual averages	Trends (% decade^{-1}) in the data	Forced trends in UV data (% decade^{-1})	
			EUV	TUV
Total ozone (DU)	330.6 ± 39.9	7.2 ± 1.7 (all sky)	−8.4 ± 2.5	−2.5 ± 1.0
		6.2 ± 5.9 (clear sky)	−7.4 ± 7.6	−1.2 ± 1.6
AOD at 320 nm	1.11 ± 0.63	22.4 ± 8.4 (all sky)	−4.7 ± 2.0	−4.7 ± 2.0
		25.3 ± 6.6 (clear sky, AOD < 0.8)	−7.3 ± 2.4	−7.3 ± 2.4
CC (%)	4.2 ± 2.9	52.4 ± 9.6	−6.3 ± 1.6	−6.8 ± 2.1
EUV (kJ m^{-2})	1.74 ± 1.1	−29.6 ± 6.2 (all sky)	—	—
		−20.8 ± 15.6 (clear sky)		
TUV (MJ m^{-2})	0.69 ± 0.33	−39.2 ± 5.6 (all sky)	—	—
		−6.0 ± 12.2 (clear sky)		
GS (MJ m^{-2})	13.8 ± 6.5	−28.6 ± 4.3 (all sky)	−20.3 ± 3.3	−20.3 ± 4.0
		−7.3 ± 11.6 (clear sky)	−5.6 ± 9.2	−4.9 ± 8.1

b. *Long-term (2004–10) characteristics*

Table 3 shows trends for the period of 2004–10 in the UV forcing factors in the fractional deviation from the reference value and trends in the UV irradiance caused by these factors. The annual-mean O_3 for 2004–10 has been increased slightly from the past value of 322 DU for 1985–2000 (Cho et al. 2003) to 330.6 ± 39.9 DU with a maximum of 380.7 DU in March and a minimum of 290.8 DU in September and October. Annual-mean AOD at 320 nm and CC are 1.11 ± 0.63 and 4.2 ± 2.9, respectively, with an apparent seasonal cycle. The AOD varies in the range of 0.58–1.85 with a maximum of 1.61 in June and a minimum of 0.86 in September. The CC ranges between 2.9 in January and 6.7 in July. The mean values of daily EUV and TUV are 1.74 ± 1.1 kJ m^{-2} and 0.69 ± 0.33 MJ m^{-2}, respectively, whereas the mean value of GS is 13.8 MJ m^{-2} (159.7 W m^{-2}) in the same period. As shown in Table 3 and Fig. 2, all the UV forcing factors tend to show increase for the period of 2004–10, with trends of +7.2%, +22.4%, and +52.4% decade^{-1} for O_3, AOD, and CC, respectively. These trends are statistically significant for O_3 only at $P < 0.001$, but are insignificant for AOD and CC. Long-term changes in O_3 have been discussed in several recent World Meteorological Organization reports and previous work (e.g., Newchurch et al. 2003; Reinsel et al. 2002; Weatherhead et al. 2000; WMO 2011; Zerefos et al. 2012). Under all-sky conditions, the trends for EUV, TUV, and GS for the same period were −29.6%, −39.2%, and −28.6% decade^{-1}, respectively. The recent decreasing trends of the UV irradiances can be mainly attributed to the recent increase in O_3, AOD, and especially CC. The forced trends are calculated by multiplying the trends of the UV forcing factors and the linear RAFs are listed in Table 3. The O_3 increase of +7.2% decade^{-1} induces a negative trend of −8.4% decade^{-1} in the EUV and −2.5% decade^{-1} in the TUV. The AOD increase of +22.4% decade^{-1} induces negative trends of 4.7% decade^{-1} in both EUV and TUV, and a simultaneous increase of CC by +52.4% decade^{-1} induces a negative trend of −6.3% decade^{-1} in the EUV and −7.3% decade^{-1} in the TUV. Thus comparatively, the large changes in long-term cloud cover by over 50% do not significantly influence daily UV changes in climatological aspects. A negative trend in GS (−28.6% decade^{-1}) as a proxy for the combined AOD and CC effects forces a decreasing trends of −20.3% decade^{-1} in both EUV and TUV. Similar analysis for the clear-sky conditions (CC < 2.5 tenths) is carried out and the results are listed in the third column of Table 3 where appropriate. Clear-sky conditions were selected for the days with CC < 2.5 tenths and AOD (320 nm) less than 0.8, to select meaningful trends with enough number of measurements in a megacity, Seoul, while not changing the basic trends. The clear-sky trend for the O_3, AOD, EUV, TUV, and GS is 6.2%, 25.3%, −20.8%, −6.0%, and −7.3% decade^{-1}, respectively. Thus, the all-sky trends are stronger than the clear-sky trends for EUV, TUV, and GS, which can be explained by the noticeable increase in CC in 2009 and 2010 in particular. The calculated trends do not match well with the observed one with reasonable accuracy because of the limited R^2 value and the nonlinear behavior among the parameters as mentioned above.

Figure 3a shows the fractional deviations of daily EUV irradiance after the removal of the AOD and CC variations from the EUV data versus that of the O_3 deviation for clear-sky conditions. Figure 3b shows similar relations for the EUV with the AOD. The straight-line fit in the figure shows that sensitivities of daily EUV irradiance to changes of O_3 (Fig. 3a) and AOD (Fig. 3b) are almost constant over the whole range of O_3 and AOD variability, respectively. From the linear regression model shown in Fig. 3, it can be estimated

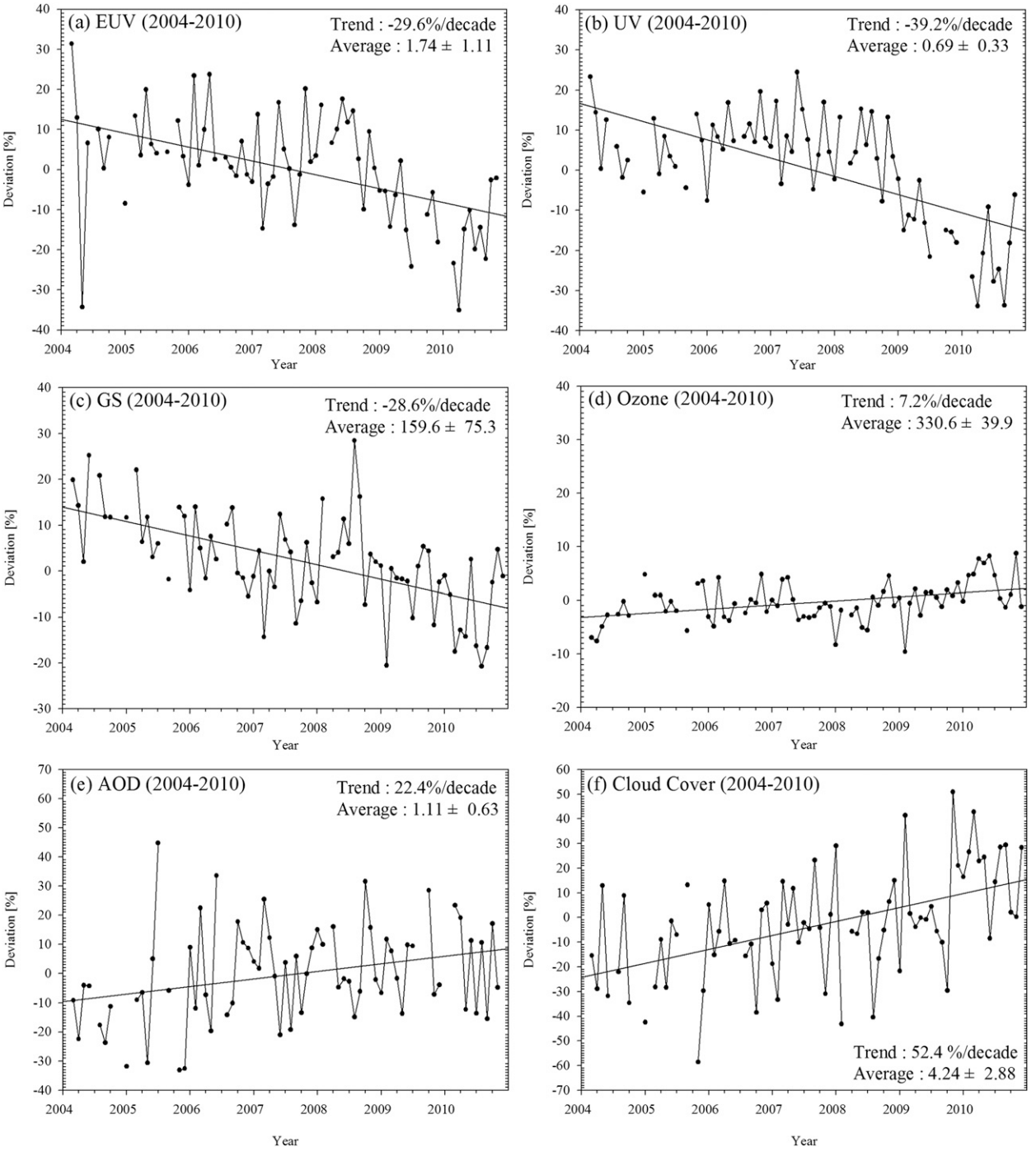

FIG. 2. Long-term trends of (a) EUV, (b) TUV, (c) GS, (d) total ozone, (e) AOD, and (f) CC for 2004–10.

that the EUV irradiance change associated with both the full ranges of observed change in O_3 (245–510 DU) and AOD (0.10–4.0) occurs at about 30%–40% of reference values (330 DU for O_3 and 1.1 for AOD) in both cases. The EUV changes of 30%–40% are larger than the estimation of 20%–30% in Belsk, Poland (Krzyscin and Puchalski 1998), which suggests the different climatology of the two locations.

c. *Radiative transfer model*

The maximum variations of the EUV irradiance at the ground due to changes in the nearly extreme O_3 and AOD

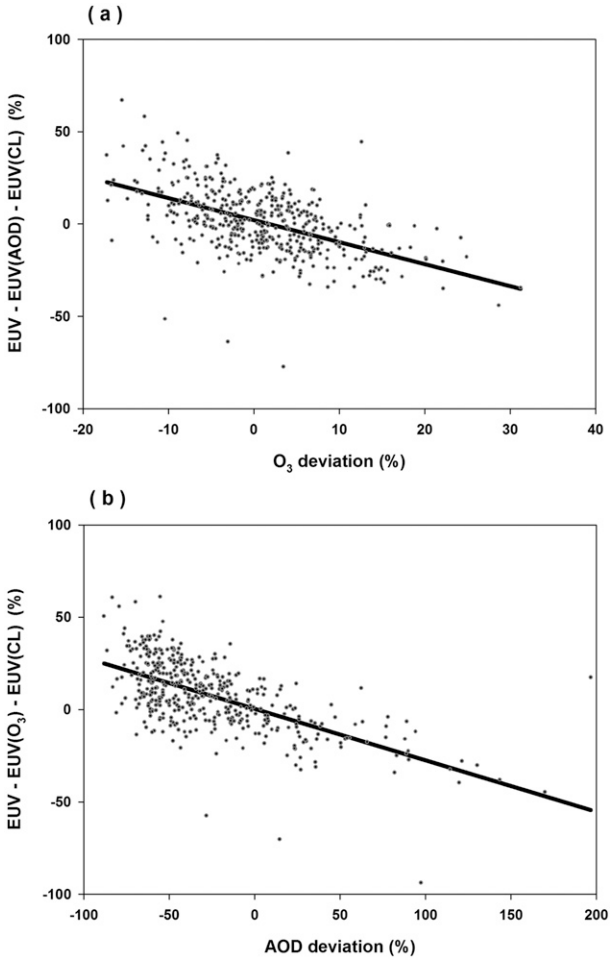

FIG. 3. The fractional deviation of the EUV daily irradiance after removal of (a) the AOD and CC variations vs that of total ozone and (b) the total ozone and CC variations vs that of AOD.

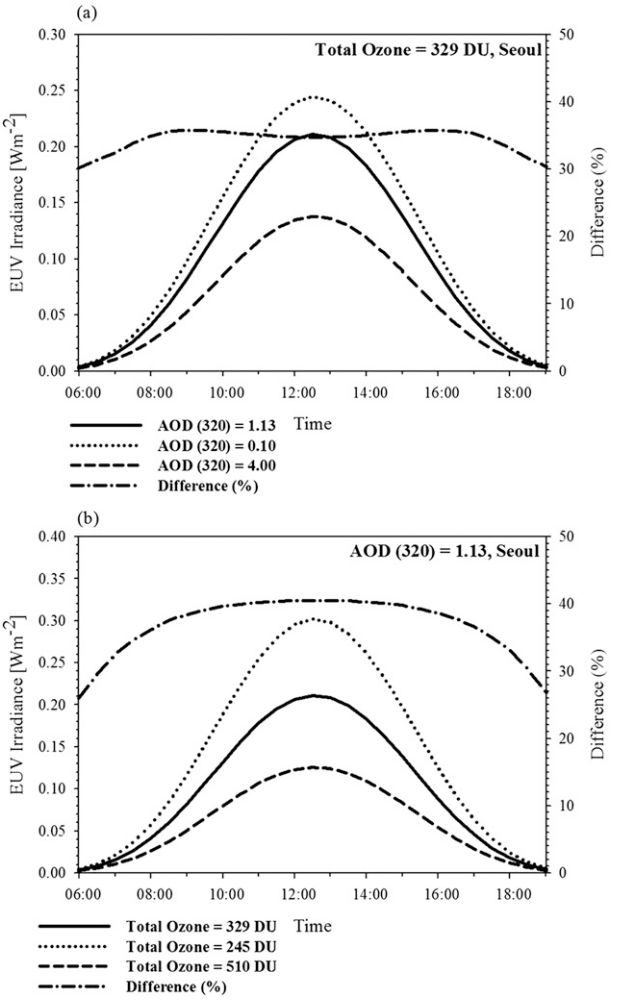

FIG. 4. The radiative transfer model (NCAR-TUV) profile of EUV irradiance on 21 Jun for (a) AOD at 320 nm and (b) total ozone, and their differences from the reference (mean value) indicating possible extreme changes in Seoul's ozone and aerosol (right axis).

under clear-sky conditions at Seoul were calculated using the tropospheric-ultraviolet and visible [National Center for Atmospheric Research (NCAR)-TUV] radiative transfer model, version 4.1, in the pseudospherical four-stream discrete ordinates mode (Madronich et al. 1998). The input for the NCAR-TUV model comprises a fixed set of atmospheric parameters adopted from Van Weele et al. (2000). The single scattering albedo of 0.98 and the asymmetry parameter of 0.7 for aerosols in the boundary layer are used here with the aerosol profile by Elterman (1968). A surface albedo of 0.03 was used, where small variations in the surface albedo affect the model results marginally (Weihs and Webb 1997). The scaling of the extinction cross section is described by the angstrom parameter (α = 0.844) and the AOD (1.13) at the wavelength of 320 nm: these values are close to the average values found in Seoul from direct sunlight observation by Koo et al. (2007). As shown in Figs. 4a and 4b, the model runs for the daily EUV irradiance for the mean values of O_3 (329 DU) and AOD (1.13) as a reference for this day, with different extremes in the maximum values of 510 DU for O_3 and 4.00 for AOD, and in the minimum values of 245 DU for O_3 and 0.10 for AOD, respectively, on 21 June. The difference between the irradiances for the extremes of O_3 and AOD, and for long-term reference is from 30% to 40%, representing a nearly constant value through the daytime. Thus the difference is almost independent of SZAs in the diurnal variation. The extreme changes in daily EUV irradiance estimated by means of the regression model (Fig. 3) correspond with those calculated using the radiative transfer model. Thus, these estimates are in reasonable agreement with the regression and radiative transfer model results.

5. Summary and conclusions

Spectral measurements of solar ultraviolet (UV) radiations by Brewer spectrophotometer were used in conjunction with total ozone measurements by Dobson spectrophotometer in Seoul during 2004–10 to investigate the relative influences and trends of the UV forcing factors of O_3, AOD and CC, and GS, together with their climatological features. The recent annual-mean O_3 has increased slightly from the past value of 322 DU (1985–2000) to 330.6 ± 39.9 DU with a monthly-mean maximum of 380.7 DU in March and a minimum of 290.8 DU in September and October. Annual-mean AOD was 1.11 ± 0.63 with a monthly-mean maximum of 1.61 in June and minimum of 0.86 in November, whereas the CC was 4.2 ± 2.9 with a monthly-mean maximum of 6.7 in July and a minimum of 2.9 in January and February. The long-term O_3 increase of +7.2% decade^{-1} induces a negative trends of −8.4% decade^{-1} in the surface EUV and of −2.5% decade^{-1} in the TUV. The AOD increase of +22.4% decade^{-1} induces a negative trends of −4.7% decade^{-1} in both EUV and TUV, and at the same time an increase of CC by +52.4% decade^{-1} induces a negative trends of −6.3% decade^{-1} in the EUV and −6.8% decade^{-1} in the TUV. Thus, comparatively, the large changes in long-term CC by more than 50% do not significantly influence daily UV changes for its low sensitivity. A negative trend in GS (−28.6% decade^{-1}) as a proxy for the combined AOD and CC effects forces a decreasing trend of −20.3% decade^{-1} in both EUV and TUV. The mean range of UV disturbances due to AOD variability is about 11% in both UV irradiances but that due to O_3 is 3% in TUV irradiance as compared with 9% in EUV irradiance. The range of the disturbances due to changes in the CC is about 7% for both UV irradiances.

The UV sensitivities to changes of the UV forcing factors from the linear RAFs and their contributions to the transmission of UV through the atmosphere have been analyzed on the basis of the multiple linear regression analyses in daily fractional deviation time series of the forcing factors from the reference values. From the linear RAF (EUV sensitivities) of O_3, AOD, CC, and GS corresponding to the regression coefficients in the year-round regression models, EUV daily irradiance in a 1% change of UV forcing factors changes by −1.16% in O_3, −0.21% in AOD, −0.12% in CC, and +0.71% in GS. Similarly, for TUV sensitivities, the TUV daily irradiance changes with similar values to EUV except for −0.35% in O_3. Although the partial correlation coefficients between both UV irradiance and AOD are higher than those between the UV and O_3, the UV sensitivity to the O_3 forcing factor is about 5 times as high as AOD. A 1% increase of GS has been found to induce a 0.7% increase in both EUV and TUV radiation, which is consistent with previous research (Krzyscin 1996). Both EUV and TUV sensitivities to aerosol changes are almost the same with a year-round value of −0.21 for all seasons. A negligible small difference between sensitivity of EUV and TUV to cloud and aerosol changes are also found for each season. The EUV model (1) using O_3, AOD, and CC explains only 49% of the variance of the daily fractional deviations of the EUV irradiance with the individual contributions of 11%, 25%, and 13%, whereas the TUV model (1) explains 53% of the variance with the respective contributions of 0.7%, 32%, and 20%. The EUV model (2) using O_3 and the GS used as a proxy for the combined EUV changes induced by cloud cover and atmospheric turbidity variations explains 61% of the EUV variance with the individual contributions of 10% and 51%, whereas the TUV model (2) explains 68% of the variance with respective contributions of 1% and 67%, with negligible effects for O_3. On the basis of the multiple analyses, we found that the UV sensitivity to O_3 is the highest among the forcing factors, but contributions of the UV forcing factors to the daily UV variability and the range of UV disturbances due to the AOD variability are affected more by AOD than by O_3 and CC in both UV fractional changes. Further studies will demonstrate that part of the UV variability that remains left to be explained, as mentioned above, could be clarified by considering new forcing factors unavailable for this climatological study.

The linear regression model for clear skies shows that the extreme values of O_3 and AOD in the Seoul record (2004–10) are associated with 30%–40% changes in daily EUV irradiance. This estimate is in reasonable agreement with the radiative transfer model calculations.

Acknowledgments. This work was funded by the Korea Meteorological Administration Research and Development Program under Grant CATER 2012-2065.

REFERENCES

Antón, M., A. Serrano, M. L. Cancillo, and J. A. García, 2008: Total ozone and solar erythemal irradiance in southwestern Spain: Day-to-day variability and extreme episodes. *Geophys. Res. Lett.,* **35,** L20804, doi:10.1029/2008GL035290.

——, L. Alados-Arboledas, J. L. Guerrero-Rascado, M. J. Costa, J. C. Chiu, and F. J. Olmo, 2012a: Experimental and modeled UV erythemal irradiance under overcast conditions: The role of cloud optical depth. *Atmos. Chem. Phys.,* **12,** 11 723–11 732.

——, A. A. Piedehierro, L. Alados-Arboledas, E. Wolfran, and F. J. Olmo, 2012b: Extreme ultraviolet index due to broken clouds at a midlatitude site, Granada (southeastern Spain). *Atmos. Res.,* **118,** 10–14.

Arola, A., K. Lakkala, A. Bais, J. Kaurola, C. Meleti, and P. Taalas, 2003: Factors affecting short- and long-term changes of spectral UV irradiance at two European stations. *J. Geophys. Res.,* **108,** 4549, doi:10.1029/2003JD003447.

Bais, A. F., C. S. Zerefos, C. Meleti, I. C. Ziomas, and K. Tourpali, 1993: Spectral measurements of solar UVB radiation and its relations to total ozone, SO_2, and clouds. *J. Geophys. Res.,* **98,** 5199–5204.

Blumthaler, M., 1993: Solar measurements. *UV-B Radiation and Ozone Depletion: Effects on Humans, Animals, Plants, Microorganisms, and Materials,* Lewis Publishers, 71–94.

Booth, C. R., and S. Madronich, 1994: Radiation amplification factors: Improved formulation accounts for large increases in ultraviolet radiation associated with Antarctic ozone depletion. *Antarct. Res. Ser.,* **62,** 39–42.

Calbó, J., D. Pagès, and J. A. González, 2005: Empirical studies of cloud effects on UV radiation: A review. *Rev. Geophys.,* **43,** RG2002, doi:10.1029/2004RG000155.

Cheymol, A., and H. De Backer, 2003: Retrieval of the aerosol optical depth in the UV-B at Uccle from Brewer ozone measurements over a long time period 1984–2002. *J. Geophys. Res.,* **108,** 4800, doi:10.1029/2003JD003758.

Cho, H. K., H. J. Kwon, and C. Y. Choi, 1998: Increase of the surface erythemal ultraviolet-B radiation by the ozone layer depletion. *Asia-Pac. J. Atmos. Sci.,* **34,** 272–281.

——, M. J. Jeong, J. Kim, and Y. J. Kim, 2003: Dependence of diffuse photosynthetically active solar irradiance on total optical depth. *J. Geophys. Res.,* **108,** 4267, doi:10.1029/2002JD002175.

——, J. Kim, Y. Jung, Y. G. Lee, and B. Y. Lee, 2008: Recent changes in downward longwave radiation at King Sejong Station, Antarctica. *J. Climate,* **21,** 5764–5776.

Elterman, L., 1968: UV, visible, and IR attenuation for altitudes to 50 km. Air Force Cambridge Research Laboratories, Environmental Research Papers 285, AFCRL-68-0153, 56 pp. [Available online at http://www.dtic.mil/cgi-bin/GetTRDoc?AD=AD0671933.]

Grobner, J., R. Vergaz, V. E. Cachorro, D. V. Henriques, K. Lamb, A. Redondas, J. M. Vilaplana, and D. Rembges, 2001: Intercomparison of aerosol optical depth measurements in the UVB using Brewer spectrophotometers and a Li-Cor spectrophotometer. *Geophys. Res. Lett.,* **28,** 1691–1694.

Herman, J. R., 2010: Global increase in UV irradiance during the past 30 years (1979–2008) estimated from satellite data. *J. Geophys. Res.,* **115,** D04203, doi:10.1029/2009JD012219.

Josefsson, W., and T. Landelius, 2000: Effect of clouds on UV irradiance: As estimated from cloud amount, cloud type, precipitation, global radiation and sunshine duration. *J. Geophys. Res.,* **105,** 4927–4935.

Jung, Y. J., H. K. Cho, J. Kim, Y. J. Kim, and Y. M. Kim, 2011: The effects of clouds on enhancing surface solar irradiance. *Atmos. Korean Meteor. Soc.,* **21,** 131–142.

Kazadzis, S., and Coauthors, 2007: Nine years of UV aerosol optical depth measurements at Thessaloniki, Greece. *Atmos. Chem. Phys.,* **7,** 2091–2101.

Kim, J., S. S. Park, K. J. Moon, J. H. Koo, Y. G. Lee, K. Miyagawa, and H. K. Cho, 2007: Automation of Dobson spectrophotometer (No. 124) for ozone measurements. *Atmos. Korean Meteor. Soc.,* **17,** 339–348.

——, ——, N. Y. Cho, W. G. Kim, and H. K. Cho, 2011: Recent variations of UV irradiance at Seoul 2004–2010. *Atmos. Korean Meteor. Soc.,* **21,** 429–438.

——, H. K. Cho, J. Mok, H. D. Yoo, and N. Cho, 2013: Effects of ozone and aerosol on surface UV radiation variability. *J. Photochem. Photobiol.,* **119B,** 46–51.

Komhyr, W. D., 1980: Operations handbook—Ozone observations with a Dobson spectrophotometer. World Meteorological Organization Global Ozone Research and Monitoring Project Rep. 6, 125 pp. [Available from Sales and Distribution of Publications, 7 bis avenue de la Paix, P.O.B. 2300, CH-1211 Geneva 2, Switzerland.]

Koo, J. H., J. Kim, M. J. Kim, H. K. Cho, K. Aoki, and M. Yamano, 2007: Analysis of aerosol optical properties in Seoul using skyradiometer observation. *Atmos. Korean Meteor. Soc.,* **17,** 407–420.

Krzyscin, J. W., 1996: UV controlling factors and trends derived from the ground-based measurements taken at Belsk, Poland, 1976–1994. *J. Geophys. Res.,* **101,** 16 797–16 805.

——, and S. Puchalski, 1998: Aerosol impact on the surface UV radiation from the ground-based measurements taken at Belsk, Poland, 1980–1996. *J. Geophys. Res.,* **103,** 16 175–16 181.

Kyle, T. G., 1991: *Atmospheric Transmission, Emission, and Scattering.* Pergamon, 288 pp.

Liou, K. N., 1992: *Radiation and Cloud Processes in the Atmosphere: Theory, Observation, and Modeling.* Oxford Monographs on Geology and Geophysics, Oxford University Press, 504 pp.

Liu, S. C., S. A. Mckeen, and S. Madronich, 1991: Effect of anthropogenic aerosols on biologically active ultraviolet radiation. *Geophys. Res. Lett.,* **18,** 2265–2268.

Lubin, D., and J. E. Frederick, 1991: The ultraviolet radiation environment of the Antarctic Peninsula: The roles of ozone and cloud cover. *J. Appl. Meteor.,* **30,** 478–493.

Madronich, S., 1992: Implications of recent total atmospheric ozone measurements for biologically active ultraviolet radiation reaching the earth's surface. *Geophys. Res. Lett.,* **19,** 37–40.

——, 1993: The atmosphere and UV-B radiation at ground level. *Environmental UV Photobiology,* Plenum Press, 1–39.

——, R. L. McKenzie, L. O. Bjorn, and M. M. Caldwell, 1998: Changes in biologically active ultraviolet radiation reaching the Earth's surface. *J. Photochem. Photobiol.,* **46B,** 5–19.

McKenzie, R. L., W. A. Matthews, and P. V. Johnston, 1991: The relationship between erythemal UV and ozone, derived from spectral irradiance measurements. *Geophys. Res. Lett.,* **18,** 2269–2272.

——, M. Blumthaler, C. R. Booth, S. B. Diaz, J. E. Frederick, T. Ito, S. Madronich, and G. Seckmeyer, 1994: Surface ultraviolet radiation. Scientific depletion of ozone: 1994. World Meteorological Organization Rep. 37, 9.1–9.22. [Available online at http://www.esrl.noaa.gov/csd/assessments/ozone/1994/chapters/chapter9.pdf.]

McKinlay, A. F., and B. L. Diffey, 1987: A reference action spectrum for ultraviolet induced erythema in human skin. *Comput. Ind. Eng.,* **6,** 17–22.

Meleti, C., and F. Cappellani, 2000: Measurements of aerosol optical depth at Ispra: Analysis of the correlation with UV-B, UV-A, and total solar irradiance. *J. Geophys. Res.,* **105,** 4971–4978.

Micheletti, M. I., R. D. Piacentini, and S. Madronich, 2003: Sensitivity of biologically active UV radiation to stratospheric ozone changes: Effects of action spectrum shape and wavelength range. *Photochem. Photobiol.,* **78,** 456–461.

Mims, F. M., and L. E. Frederick, 1994: Cumulus clouds and UV-B. *Nature,* **371,** 291–291.

Newchurch, M. J., E.-S. Yang, D. M. Cunnold, G. C. Reinsel, J. M. Zawodny, and J. M. Russell, 2003: Evidence for slowdown in stratospheric ozone loss: First stage of ozone recovery. *J. Geophys. Res.,* **108,** 4507, doi:10.1029/2003JD003471.

Reinsel, G. C., E. C. Weatherhead, G. C. Tiao, A. J. Miller, R. M. Nagatani, D. J. Wuebbles, and L. E. Flynn, 2002: On detection of turnaround and recovery in trend for ozone. *J. Geophys. Res.,* **107** (D10), doi:10.1029/2001JD000500.

Sabburg, J., and J. Wong, 2000: Evaluation of a sky/cloud formula for estimating UV-B irradiance under cloudy skies. *J. Geophys. Res.,* **105,** 29 685–29 691.

Schafer, J. S., V. K. Saxena, B. N. Wenny, W. Barnard, and J. J. DeLuisi, 1996: Observed influence of clouds on ultraviolet-B radiation. *Geophys. Res. Lett.,* **23,** 2625–2628.

Stolarski, R., R. Bojkov, L. Bishop, C. Zerefos, J. Staehelin, and J. Zawodny, 1992: Measured trends in stratospheric ozone. *Science,* **256,** 342–349.

Van Weele, M., and Coauthors, 2000: From model intercomparison toward benchmark UV spectra for six real atmospheric cases. *J. Geophys. Res.,* **105,** 4915–4925.

Weatherhead, E. C., and Coauthors, 2000: Detecting the recovery of total column ozone. *J. Geophys. Res.,* **105,** 4915–4925.

Weihs, P., and A. R. Webb, 1997: Accuracy of spectral UV model calculations. 1. Consideration of uncertainties in input parameters. *J. Geophys. Res.,* **102,** 1541–1550.

Wilks, D. S., 2006: *Statistical Methods in the Atmospheric Sciences.* International Geophysics Series, Academic Press, 704 pp.

WMO, 2011: Scientific assessment of ozone depletion: 2010. Global Ozone Research and Monitoring Project, Rep. 52, 516 pp. [Available online at http://www.esrl.noaa.gov/csd/assessments/ozone/2010/.]

Zerefos, C. S., K. Tourpali, K. Eleftheratos, S. Kazadzis, C. Meleti, U. Feister, T. Koskela, and A. Heikkilä, 2012: Evidence of a possible turning point in solar UV-B over Canada, Europe and Japan. *Atmos. Chem. Phys.,* **12,** 2469–2477.